Photochemistry of 124-Kilodalton *Avena* Phytochrome under Constant Illumination in Vitro†

John M. Kelly and J. Clark Lagarias*
Department of Biochemistry and Biophysics, University of California at Davis, Davis, California 95616
Received February 1, 1985

ABSTRACT: The action of continuous red and far-red illumination on the kinetics of phototransformations between red- and far-red-absorbing forms (P_R and P_{FR}, respectively) of 124-kilodalton *Avena* phytochrome in vitro was determined with a new experimental approach. With this method, light-induced absorbance changes measured as a function of absorbed fluence afforded the determination of the photochemical cross sections for the two phytochrome phototransformations. The quantum yields of 0.152 ± 0.008 mol einstein^{-1} for the conversion of P_R to P_{FR} under red illumination (ϕ_R) and 0.069 ± 0.004 mol einstein^{-1} for the P_{FR} to P_R photoconversion under far-red illumination (ϕ_{FR}) were determined from these measurements. The quantum yield ratio (ϕ_R/ϕ_{FR}) of 2.20 ± 0.01 was found to be significantly larger than that previously reported for *Avena* phytochrome in vitro. The mole fraction of P_{FR} observed at photoequilibrium under continuous red light illumination was estimated to be 0.876 ± 0.006. These results have been used to predict the absorption spectrum of the P_{FR} form and the wavelength dependence of the photoequilibrium produced under continuous illumination throughout the visible and near-ultraviolet spectra.

The biliprotein phytochrome mediates a wide range of red-light-induced developmental responses in plants (Shropshire & Mohr, 1983; Schopfer, 1984). Physiological studies support the hypothesis that the action of light on plant development is primarily determined by the equilibrium mixture of the two photointerconvertible forms of phytochrome, the red-absorbing form (P_R)[1] and the far-red-absorbing form (P_{FR}), established by continuous illumination of the plant. For this reason, considerable interest has focused on characterization of the P_R to P_{FR} and P_{FR} to P_R photoprocesses in vitro. Numerous studies have shown that two significant transformations accompany each of the light-driven $P_R \rightleftharpoons P_{FR}$ conversions—a primary photoprocess involving the linear tetrapyrrolic prosthetic group which occurs on the picosecond time scale (Song et al., 1979; Wendler et al., 1984) and a subsequent series of light-independent rearrangements of the protein backbone which occur on the nanosecond to second time scale (Linschitz et al., 1966; Kendrick & Spruit, 1977; Pratt et al., 1984). The latter processes are believed to be responsible for initiating the sequence of biophysical and biochemical events which lead to phytochrome-mediated photomorphogenesis in plants.

Renewed interest in characterizing the photochemical properties of phytochrome has come from recent evidence that the native chromoprotein is susceptible to a limited proteolytic cleavage of a terminal 4–6-kDa segment (Vierstra & Quail, 1982). The observation that the native 124-kDa species isolated from etiolated *Avena* seedlings exhibits considerably different spectrophotometric properties from the more degraded species previously isolated, particularly for the P_{FR} form, has led to the hypothesis that this 4–6-kDa region plays an important role in stabilizing the conformation of the P_{FR} phytochrome molecule (Vierstra & Quail, 1983b, Litts et al., 1983). Although an initial study of the photochemistry of the 124-kDa species has been presented (Vierstra & Quail, 1983a), the present work was initiated to develop a new methodology to quantitatively evaluate the kinetics of the overall interconversions of the 124-kDa species under defined experimental conditions. Our analysis of the phytochrome phototransformations is based upon the work of Johns (1969), who applied this approach to equilibrium concept to the quantum yield determination of the photochromic pyrimidine–pyrimidine dimer system of nucleic acids. This method sharply contrasts with the initial rates analysis developed by Butler et al. (1964) by combining rigorous light intensity measurements with the ability to rapidly follow the complete $P_R \rightleftharpoons P_{FR}$ phototransformations across a wide range of optical density. We report here the quantum yields for the two phototransformations of the 124-kDa species from etiolated *Avena* seedlings and the equilibrium mole fraction of P_{FR} produced under continuous illumination with red light, using both the approach to equilibrium method and the initial rates method of analysis. With special attention to the assumptions and advantages of each method, the results of previous photochemical measurements on *Avena* phytochrome are compared with these measurements.

Materials and Methods

Chemical Reagents. All aqueous solutions and buffers were prepared with water purified by a Milli-Q water purification system (Millipore Corp.). All glassware was washed with 3 M HNO_3 and rinsed extensively with Milli-Q water before use. All chemicals used were reagent grade. Potassium ferrioxalate, $K_3Fe(C_2O_4)_3$, was prepared according to Calvert & Pitts (1967) and made anhydrous by drying in vacuo over P_2O_5. Anal. Calcd for $C_6O_{12}K_3Fe$: C, 16.48; H, 0; N, 0.

† This study was supported by research grants from the National Science Foundation (PCM81-08090 and PM84-09074). J.M.K. was the recipient of a Jastro-Shields graduate fellowship (University of California, Davis).
* Correspondence should be addressed to this author.

[1] Abbreviations: P_R, red-light-absorbing form of phytochrome; P_{FR}, far-red-light-absorbing form of phytochrome; SAR, specific absorbance ratio (ratio of A_{668}/A_{280} for P_R); SDS–PAGE, sodium dodecyl sulfate–polyacrylamide gel electrophoresis; M_r, relative molecular weight; E, einstein (mole of photons); EDTA, ethylenediaminetetraacetic acid; TEGE buffer, 0.025 M Tris-HCl, 4.0 M ethylene glycol, and 0.001 M EDTA, pH 7.8 at 5 °C; Tris-HCl, tris(hydroxymethyl)aminomethane hydrochloride; kDa, kilodalton(s).

0006-2960/85/0424-6003$01.50/0

Found: C, 16.27; H, 0.13; N, 0.15. Ferrioxalate crystals and 0.15 M solutions in 0.1 N H_2SO_4 were stored at room temperature in complete darkness. Reinecke's salt, $KCr(NH_3)_2(NCS)_4$, was prepared according to Wegner & Adamson (1966). Anal. Calcd for $C_4H_6N_6S_4KCr$: C, 13.44; H, 1.69; N, 23.51. Found: C, 13.52; H, 2.79; N, 25.37.

Phytochrome Preparations. Undegraded 124-kDa phytochrome was purified as P_R from etiolated oat seedlings according to the method of Litts et al. (1983) with the modifications described by Lagarias & Mercurio (1985). The phytochrome samples used for photochemical measurements were judged to be >95% pure by gradient SDS–PAGE (Laemmli, 1970) and exhibited a predominant monomer molecular weight of 124000 with small amounts of a 121-kDa species on gradient gels. The specific absorbance ratio (SAR) of the phytochrome samples ranged between 0.95 and 1.10. With the exception of variability in the amount of dark reversion of the samples (2–15% loss of absorbance at 730 nm for P_{FR} over a 12-h period at 5 °C), the spectrophotometric properties of these phytochrome samples were identical with those previously reported (Litts et al., 1983). Before photochemical measurements, phytochrome samples, stored at −80 °C in TEGE buffer (0.025 M Tris-HCl, 4.0 M ethylene glycol, and 1 mM EDTA, pH 7.8 at 5 °C), were thawed to 5 °C and diluted to the desired concentration with fresh TEGE buffer at 5 °C.

Irradiation and Measuring Geometry. Figure 1 illustrates the geometric arrangement of the actinic source, the measuring source, and the sample cuvette. Actinic irradiation was provided by a 24-V, 250-W tungsten–halogen projector lamp with an integral dichroic reflector (Sylvania type EMM). Lamp voltage was controlled by means of a 110 V:110 V voltage-regulated transformer (Sola) in series with a variable stepdown transformer (Variac) and a 110 V:24 V fixed stepdown transformer. Monochromatization was provided by narrow band-pass three-cavity interference filters (7–11-nm half-bandwidth, Ditric Optics) placed in front of the focusing lens. The actinic beam illuminated an open quartz cuvette from above, with the cuvette lying completely inside the 5-cm diameter beam. The measuring beam of the Hewlett Packard HP8450A spectrophotometer was oriented normal to the actinic beam, giving a measuring path length (b_0) of 1 cm. All irradiations utilized a 2.0-mL sample volume which was rapidly stirred throughout the experiment. This volume gives a geometric actinic path length (b) of 2 cm (see later discussion). Temperature control (±0.1 °C) of the sample was afforded by an HP89000A temperature control station. For light intensity measurements, light from the irradiation source was directed into the spectrophotometer diode array with a quartz fiber optic cable (6.5-mm bundle diameter, 30-cm length; Dolan Jenner). All absorbance and intensity measurements with the HP8450A instrument were made with a fixed wavelength resolution of 2 nm.

Light Intensity Measurements. Potassium ferrioxalate actinometry, first described by Hatchard & Parker (1956), was used to measure the incident light intensity (I_0^i) within the sample cuvette of our irradiation system. Because the utility of the ferrioxalate actinometer is confined to the blue region of the visible spectrum, a method to use the diode array of the HP8450A was devised to measure visible light intensities outside this spectral region. Calibration of the diode array to measure absolute light intensities was a two-step process. First, the relative responses of the diodes were measured by directing the output of a calibrated tungsten lamp (Perkin Elmer 065-0550) through the quartz fiber optic cable into the diode array spectrograph of the HP8450A. The wavelength distribution of the light intensity was thus recorded. The known intensity of the calibrated light source was then divided by these measured intensity values to give the diode response correction factors as a function of wavelength. These correction factors were applied to the measured intensity distribution of the filtered actinic light source to give corrected relative (I_λ^{mc}) outputs at various wavelengths throughout the visible and near-infrared spectra. The transmission maxima of the irradiation wavelengths used for these studies included 434, 478, 543, 608, 636, 648, 657, 727, and 738 nm.

To provide an absolute intensity scale for the filtered actinic light source, the incident intensity at 434 nm was determined with 0.15 M potassium ferrioxalate actinometry (Hatchard & Parker, 1956). These measurements were performed under a red safelight (Westinghouse F15T8/CW fluorescent lamps filtered with 0.125-in. red Plexiglas, Rohm and Haas dye 2100, Caloric Color Co., Garfield, NJ). The incident light intensity (I_0^i in picoeinsteins per second) was calculated according to the detailed protocol outlined in Calvert & Pitts (1967) with the following modifications. Both solution absorbance ($\bar{A}_\lambda$) and quantum yields for ferrioxalate photoreduction ($\bar{\phi}_\lambda$) were intensity normalized across the spectral band-pass of the actinic source (i.e., 422–446 nm) at 2-nm intervals according to the method of Demas (1973). ϕ_λ values were interpolated from values reported by Hamai & Hirayama (1983). The resulting values of I_0^i provided an absolute intensity scale for the diode array monitor at 434 nm and therefore at the other wavelengths used for these studies. This calibration of the diode array was verified with a spectrally neutral 1.5 mm × 1.5 mm solid-state hot junction thermopile (Oriel Corp., 7102) outputted to a Keithley Model 149 nanovoltmeter and with Reinecke's salt actinometry performed according to the method of Wegner & Adamson (1966).

Determination of Apparent Path Length. The nonideal geometry of our irradiation facility (Figure 1) required the development of an experimental method for determining the fraction of the incident light absorbed by the sample. Although this fraction can be estimated by the expression $1 - 10^{-Ab/b_0}$ where A is the solution absorbance measured through path length b_0 and b is the path length of the irradiating beam (Johns, 1969), it assumes ideal irradiation geometry. For our system, light reflection from the sides and bottom of the sample cuvette contributed to deviations from this ideal approximation. Corrections for this effect are especially important since the optical density of phytochrome solutions changes during illumination. As the optical density of the solution decreases, the fraction of light which is reflected from the internal cuvette faces increases. To determine the magnitude of this effect on a quantitative basis, we again used solution actinometry, a true measure of absorbed dose.

The increase in the contribution of reflected light to the absorbed fluence as the solution optical density decreases can be conceptualized as an apparent increase in the length of the light path (b) through the solution. When an optically thick actinometer solution is exposed to some increment of incident fluence (L_0), the developed absorbance of the photoproduct (A_P) is given by eq 1 (Johns, 1969) where ϵ_P is the molar

$$A_P = L_0 \cdot \epsilon_P \cdot \Phi \cdot (1 - 10^{-\bar{A}_\lambda \cdot b/b_0}) \quad (1)$$

extinction coefficient of the developed photoproduct, ϕ is the actinometer quantum yield, $\bar{A}_\lambda$ is the intensity-normalized actinometer absorbance across the spectral band-pass of the actinic source with transmission maximum at wavelength λ (Demas, 1973), b_0 is the path length through which $\bar{A}_\lambda$ is

measured, and b is the geometric irradiation path length. If our system had ideal irradiation geometry, b would be equal to 2 cm for a 2.0-mL sample. When an optically thin actinometer solution (solution 2) is exposed to the same increment of incident fluence as an optically thick solution (solution 1), the ratio of the developed absorbances, $(A_P)_2/(A_P)_1$, should equal the ratio of the fractions of incident fluence absorbed by the two solutions, $[1 - 10^{-(\bar{A}_\lambda)_2 b_2/b_0}]/[1 - 10^{-(\bar{A}_\lambda)_1 b_1/b_0}]$. Since the irradiation geometry is nonideal, the apparent irradiation path length of optically thin solutions, which we will designate as $\bar{b}$, can be conceptualized to differ from the geometric irradiation path length, b. Substituting $\bar{b}$ for b_2 and b for b_1 gives the following relationship between solution absorbance and the apparent path length $\bar{b}$ for our system.

$$\bar{b} = \frac{b_0}{(\bar{A}_\lambda)_2} \cdot \log\left|1 - \frac{(A_P)_2}{(A_P)_1} \cdot (1 - 10^{-(\bar{A}_\lambda)_1 \cdot b/b_0})\right| \quad (2)$$

Because the quantum yield for the photoreduction of ferrioxalate is concentration dependent (Hatchard & Parker, 1956), the dependence of the absorbed light dose on decreasing solution absorbance was therefore determined by using the Reinecke's salt actinometer (Wegner & Adamson, 1966) with the following modifications. A stock solution of 28 mM $KCr(NH_3)_2(NCS)_4$ in ice-cold 0.1 N H_2SO_4 was filtered through a 0.45-μm Millipore-type HA filter and diluted with ice-cold 0.1 N H_2SO_4 before use. The sample cuvette was filled with 1.50 mL of appropriately diluted actinometer solution (c = 0.5–28 mM) and 0.50 mL of cold 0.32 M $Fe(NO_3)_3 \cdot 9H_2O$/1.60 M $HClO_4$ developer solution. Each solution was irradiated at 5 °C with a light fluence (L_0) of 520 ± 10 pE cm^{-2} at 543 nm as determined by the thermopile. This dose of light was shown to produce less than a 5% decrease in solution absorbance at the irradiating wavelength for all Reinecke's salt concentrations investigated. The amount of $Fe(NCS)_2^+$ photoproduct produced by this light dose for each different concentration was determined from the difference in absorbance at 450 nm before and after irradiation. An empirical relationship between the experimental values of apparent path length ($\bar{b}$), calculated according to eq 2, and the intensity-normalized absorbance ($\bar{A}_\lambda$) was then derived by nonlinear least-squares analysis.

Phototransformations of Phytochrome. All phytochrome samples used in these experiments had A_{668} between 0.3 and 0.6 in a 1-cm path length. Phytochrome solutions (2.0 mL) were transferred to the sample cuvette in the temperature-controlled station of the HP8450A and allowed to equilibrate with stirring for 5 min at 5 °C. The samples were preirradiated at 738 nm to give >98% P_R or at 648 nm to give the maximum photoequilibrium concentration of P_{FR}. The sample was then exposed to the actinic light at 648 or 738 nm for P_R to P_{FR} and for P_{FR} to P_R phototransformations, respectively. Absorbance and intensity spectra were recorded during the illumination process at fixed timed intervals ranging from 11 to 45 s. Spectral data collected during the experiments and stored on a 5.25-in. floppy disk were subsequently transferred to a separate IBM PC microcomputer for analysis.

Photochemical measurements by the method of initial rates (Butler et al., 1964) were performed on a Cary 14 spectrophotometer with temperature control at 0 °C. Phytochrome samples (5.5 mL) in 10 cm long × 0.5 cm diameter cylindrical cuvettes were irradiated at right angles to the direction of the measuring beam (10 cm) (Taylor & Bonner, 1967). The initial solution absorbance (A_{668}^{1cm}) was always less than 0.10. Irradiation was provided by a 500-W tungsten–halogen projector lamp equipped with a Balzer's IR stop filter and the appropriate interference and neutral density filters as described earlier. With this irradiation geometry, the light intensity at 434 nm was determined by potassium ferrioxalate actinometry (Calvert & Pitts, 1967), and absolute intensities at 648 and 738 nm were determined relative to this value as described earlier. To obtain data for the initial rates of both the P_R and P_{FR} transformations, the solution absorbance at 730 nm was recorded following successive 10–15-s increments of fluence with the total extent of phototransformation not exceeding 10%. In these initial rate experiments, photochemical parameters were calculated as described by Butler (1972).

Calculation of Photochemical Parameters for the Approach to Equilibrium Method. The photochemical cross sections (σ^R and σ^{FR}) of the phototransformations were calculated from plots of the natural logarithm of the percent initial absorbance minus the final absorbance at the irradiation wavelength λ, $\ln(100[(A_t - A_f)/(A_0 - A_f)])$, vs. the absorbed fluence $\bar{L}$ by using a method similar to that described by Johns (1969). The total fluence, $\bar{L}$ in units of microeinsteins per square centimeter, absorbed by a well-stirred sample at any point where A_t is measured was given by eq 3 where I_0^i in microeinsteins per

$$\bar{L} = \sum \left| \frac{I_0^i \cdot b_0 \cdot \Delta t \cdot 1 - e^{-2.3 \cdot \bar{A}_\lambda \cdot \bar{b}/b_0}}{2.3 \cdot \bar{A}_\lambda \cdot V} \right| \quad (3)$$

second was obtained from the calibrated diode array monitor (as described earlier), Δt was the time interval between measurements in seconds, V was the solution volume in milliliters, and $\bar{A}_\lambda$, $\bar{b}$, and b_0 were obtained as described previously. The photochemical cross section of the phototransformation (σ_λ in square centimeters per microeinstein) is defined as $1/\bar{L}_{37}$ where $\bar{L}_{37}$ is the absorbed fluence value where $100[(A_t - A_f)/(A_0 - A_f)] = 36.8$ (Johns, 1969).

For P_R transformation by red light of wavelength λ_1 and P_{FR} transformation by far-red light of wavelength λ_2, the ratio of the quantum yields was calculated as follows

$$\frac{\Phi_{\lambda_1}^R}{\Phi_{\lambda_2}^{FR}} = \frac{\sigma_{\lambda_1}^R \cdot A_{\lambda_2}^{FR\,max}}{\sigma_{\lambda_2}^{FR} \cdot A_{\lambda_1}^{R\,max}} \quad (4)$$

where $\sigma_{\lambda 1}^R$ and $\sigma_{\lambda_2}^{FR}$ are the experimentally determined photochemical cross sections and $A_{\lambda_1 max}^R$ and $A_{\lambda_2 max}^{FR}$ are the solution absorbances at λ_1 and λ_2 following saturating far-red and red illumination, respectively. This equation arises when Butler's derivation for the quantum yield ratio (Butler, 1972) is reconciled with the absorbed fluence concepts presented by Johns (1969). The mole fraction of P_{FR} at red light photoequilibrium ($X_{\lambda eq}^{FR}$) was then determined from the quantum yield ratio and the solution absorbances at λ_1 following saturating red and far-red irradiations, $A_{\lambda_1 min}^R$ and $A_{\lambda_1 max}^R$, according to Butler (1972) (cf. eq 5). Because P_R and P_{FR} both absorb red

$$X_{\lambda_1}^{FR\,eq} = 1 - \left|\frac{A_{\lambda_1}^{R\,min}}{A_{\lambda_1}^{R\,max}}\right| \cdot \left|1 + \frac{\Phi_{\lambda_1}^R}{\Phi_{\lambda_2}^{FR}}\right|^{-1} \quad (5)$$

wavelengths of light, the experimentally determined photochemical cross-section $\sigma_{\lambda_1}^R$ is the sum of two cross sections, σ^f and σ^r, representing the forward and reverse transformations of phytochrome at λ_1. Johns (1969) describes a method for deconvolution of these cross sections and calculation of the quantum yields in the approach to equilibrium system. However, because only P_{FR} absorbs significantly at far-red wavelengths (i.e., λ_2), it is simpler to first calculate the far-red quantum yield from the single-component cross-section $\sigma_{\lambda_2}^{FR}$. The far-red quantum yield ($\phi_{\lambda_2}^{FR}$) is defined as $\sigma_{\lambda_2}^{FR}/\alpha_{\lambda_2}^{FR}$, where $\alpha_{\lambda_2}^{FR}$ is the absorption cross section for P_{FR} at λ_2 in centimeters squared per micromole. This absorption cross section is de-

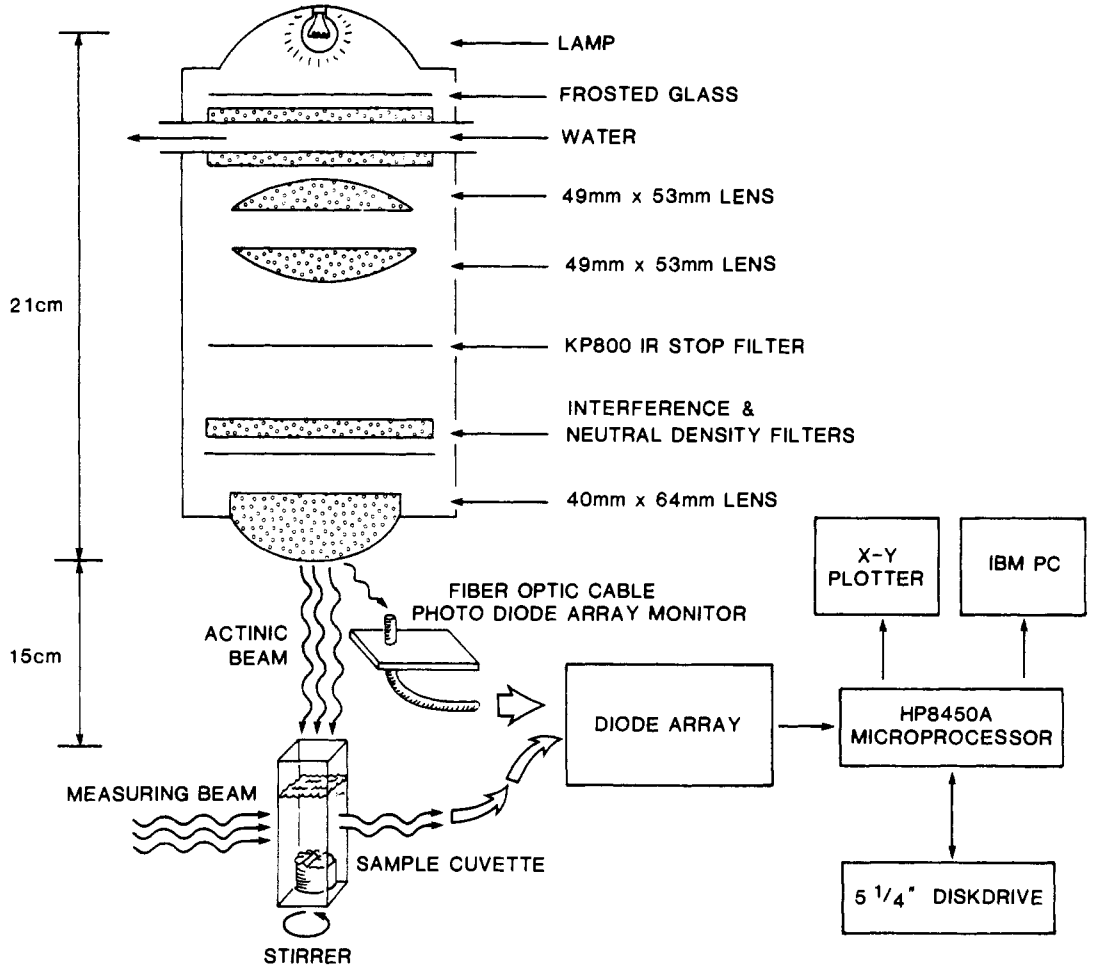

FIGURE 1: Schematic representation of the irradiation facility.

termined from $X^{FR}_{\lambda_1}$, $A^{FR}_{\lambda_2 max}$, $A^{R}_{648 max}$, and the absorption cross section of P_R at 648 nm (α^R_{648}) according to eq 6. [Note: α^R_{648}

$$\alpha^{FR}_{\lambda_2} = \frac{A^{FR}_{\lambda_2 max} \cdot \alpha^{R}_{648}}{A^{R}_{648 max} \cdot X^{FR}_{648 eq}} \quad (6)$$

$= (2.3 \times 10^{-3})\epsilon_{648} = 200$ cm^2 μmol^{-1} where ϵ_{648} is the molar extinction coefficient for the P_R form at 648 nm; see paragraph at end of paper regarding supplementary material available.] Having determined $\phi^{FR}_{\lambda_2}$, the quantum yield for the P_R to P_{FR} photoconversion ($\phi^R_{\lambda_1}$) was obtained from eq 4.

Results

An accurate and reliable method for the measurement of the dose of light absorbed by a photochemical system in solution is required for a valid determination of a quantum yield. This is especially difficult to accomplish using a flat-surface radiometric device since the contribution of reflection and refraction of light to the absorbed dose cannot reliably be predicted for most experimental systems. Under Materials and Methods, we have outlined a method to calibrate the photodiode array of the HP8450A UV–visible spectrophotometer for use as a spectroradiometer which accounts for the nonideal geometry of our irradiation facility (Figure 1).

To test the validity of this calibration of the diode array monitor, the values of the incident light intensity (I^i_0) determined with the calibrated diode array monitor were compared with those determined by thermopile and actinometric measurements at a number of wavelengths throughout the visible spectrum. Ferrioxalate actinometry at 478 nm and Reineckate actinometry at both 478 and 543 nm agreed with the diode array measurement to within 2%. These results indicate that the diode array monitor values were equivalent to a direct actinometric measurement at wavelengths other than 434 nm. The incident light intensity of the actinic source was also measured with a thermopile placed directly in the light beam. By use of the thermopile, the light intensity of the actinic source at the surface of the sample cuvette in picoeinsteins per square centimeter per second was estimated to be $0.42I^i_0$, where I^i_0 in units of picoeinsteins per second was determined as described under Materials and Methods. Even though the HP and thermopile intensity measurements had different absolute magnitudes, the magnitudes of the response of the two instruments relative to their responses at 434 nm agreed to within an aggregate error of 2% at the following irradiation wavelengths: 478, 543, 608, 636, 648, 656, 727, and 738 nm (data not shown). These results validate the calibration of the diode array monitor over the entire visible spectrum.

Figure 2 shows the results of experiments with the modified Reineckate actinometer to determine the dependence of the apparent path length ($\bar{b}$) of the irradiation system on the intensity-normalized solution absorbance ($\bar{A}_\lambda$). The function plotted through the points was determined by fitting the data to the equation $\bar{b} - b = ae^{-c\bar{A}}$ by nonlinear least-squares analysis. The values obtained for the unknown parameters were $a = 0.77$ and $c = 11.4$. The geometric path length, b, equals 2.0 cm for our irradiation system (Figure 1). Actinometry with ferrioxalate at 543 nm and with Reinecke's salt at 648 nm, wavelengths where $\bar{A}_\lambda$ was less than 0.06, agreed with the diode array measurement to within 15% (data not shown). These results support the empirical relationship of the apparent path length ($\bar{b}$) with the solution absorbance ($\bar{A}_\lambda$) since $\bar{b}$ values were used in the determinations of incident

Table I: Visible Photochemical Parameters of *Avena* Phytochrome in Vitro

	$\phi^R_{\lambda_1}$	$\phi^{FR}_{\lambda_2}$	$\phi^R_{\lambda_1}/\phi^{FR}_{\lambda_2}$	$X^{FR}_{\lambda_1 eq}$	$\epsilon^{P_R}_{\lambda max}$ (L mol^{-1} cm^{-1})	intensity (pE cm^{-2} s^{-1}) $I^i_0(\lambda_1)$	$I^i_0(\lambda_2)$
present studies (124-kDa phytochrome)[a]							
approach to equilibrium analysis[b]	0.152 ± 0.008[d]	0.069 ± 0.004[d]	2.20 ± 0.01[d]	0.876 ± 0.006[d]	121 000	≤126 (648 nm)	≤588 (738 nm)
initial rates analysis[c]	0.254[e]	0.165[e]	1.54	0.853[e]	121 000	≤126 (648 nm)	≤588 (738 nm)
previous studies[c]							
60-kDa phytochrome (Butler, 1972)	0.27 (0.13)[f]	0.18 (0.09)[f]	1.50	0.81	60 000	NR[g]	NR
60-kDa phytochrome (Pratt, 1975)	0.21 (0.13)[f]	0.15 (0.09)[f]	1.47	0.81	76 000	520 (665 nm)	750 (723 nm)
118/114-kDa phytochrome (Pratt, 1975)	0.17 (0.10)[f]	0.17 (0.10)[f]	1.00	0.75	70 000	520 (665 nm)	750 (723 nm)
118/114-kDa phytochrome (Vierstra & Quail, 1983a)	0.11 (0.07)[f]	0.12 (0.07)[f]	0.98	0.79	75 000	~300 (665 nm)	~300 (730 nm)
124-kDa phytochrome (Vierstra & Quail, 1983a)	0.17 (0.10)[f]	0.10 (0.06)[f]	1.76	0.86	73 000	~300 (655 nm)	~300 (730 nm)

[a] The present photochemical measurements employed 124-kDa *Avena* phytochrome with the following standard conditions: 2–5 μM phytochrome monomer concentration in TEGE buffer, pH 7.8 at 5 °C, using intensities I^i_0(648 nm) ≤ 300 pE s^{-1} and I^i_0(738 nm) ≤ 1400 pE s^{-1}. [b] As described under Materials and Methods. [c] Photochemical parameters were determined according to the initial rates method of Butler et al. (1964). [d] These values represent the mean of eight independent determinations and are shown with the 95% confidence limit. [e] These values represent the average of two independent determinations. [f] Values in parentheses represent quantum yields corrected for the monomer extinction coefficient determined for 124-kDa phytochrome ($\epsilon^R_{\lambda max}$ = 121 000 L mol^{-1} cm^{-1}) after Litts et al. (1983). [g] NR, not reported.

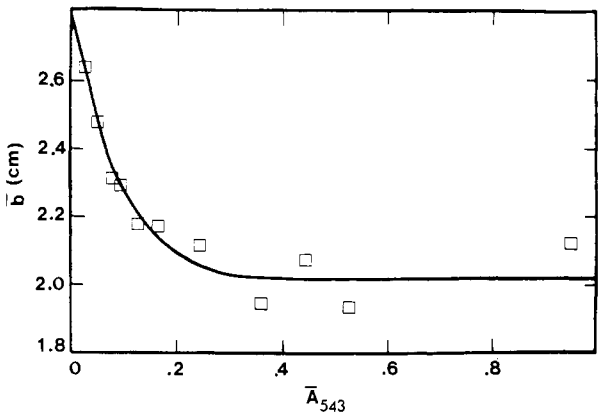

FIGURE 2: Relationship between the apparent path length ($\bar{b}$) and the intensity-normalized absorbance of Reinecke's salt actinometer solutions at 543 nm ($\bar{A}_{543}$) for our irradiation geometry. As described under Materials and Methods, the apparent path length ($\bar{b}$) for different concentrations of the Reinecke's salt actinometer was determined by using eq 2 and plotted as a function of $\bar{A}_{543}$ values (experimental values shown by squares). The curve represents the nonlinear least-squares best fit of the experimental data which are described by the expression $\bar{b} = 2.0 + 0.77\epsilon^{-11.4\bar{A}_{543}}$.

intensity (I^i_0) for the actinometer experiments.

The application of the approach to equilibrium analysis of Johns (1969) to the determination of the photochemical parameters for phytochrome required the development of standard conditions for the experimental measurements. The "standard conditions" employed for these studies include phytochrome monomer concentrations of 2–5 μM [based on ϵ^R_{668} = 121 000 L mol^{-1} cm^{-1} according to Litts et al. (1983)] in TEGE buffer at 5 °C using the following incident intensities for red and far-red illumination: I^i_0(648 nm) ≤ 300 pE s^{-1} and I^i_0(738 nm) ≤ 1400 pE s^{-1}. Figure 3 illustrates representative absorption spectra of the P_R form of phytochrome obtained after saturating irradiation at 738 nm and the photoequilibrium mixture of P_{FR} and P_R forms obtained after saturating irradiation at 648 nm under these experimental conditions. The absorbance maxima of 668 and 730 nm for the P_R form and the red-light-induced P_{FR}/P_R photoequilibrium mixture, respectively, and their relative extinction coefficients are similar to those previously reported (Litts et al., 1983; see supplementary material).

Standard conditions for the actinic light intensity were chosen to ensure that the phytochrome photointerconversions involved only two major components, P_R and P_{FR}. Since the presence of several transient light-absorbing intermediates along the $P_R \rightleftharpoons P_{FR}$ photoconversion pathways has been previously established (Linschitz et al., 1966), we chose to experimentally determine the appropriate light intensity where the contribution of the transient species to the absorption of light by the actinic irradiation was negligible. The two-component nature of our system was determined by isosbestic analysis with experimental variation of the incident light intensity (I^i_0) from 100 to 3500 pE s^{-1}. Figure 4 demonstrates measurable deviation from a two-component system during the P_R to P_{FR} photoconversion at high light intensity (2900 pE s^{-1} at 648 nm) shown by the loss of the isosbestic point at 688 nm seen at reduced light intensity (160 pE s^{-1}). This deviation was observed for intensities as low as 450 pE s^{-1}. By contrast, no loss of the two-component system was observed for the P_{FR} to P_R photoconversion measurements under 738-nm illumination with I^i_0 values as high at 3300 pE s^{-1} (Figure 4). On the basis of these results, we have utilized the actinic intensities indicated above.

Figure 5 illustrates representative plots of the phototransformations of P_R by 648-nm irradiation and P_{FR} by 738-nm irradiation as functions of absorbed fluence ($\bar{L}$) under standard conditions showing the linearity of the data obtained by this method. Numerous experiments have shown no deviation from log linearity even after 90% photoconversion in both directions. Photochemical analysis of these results according to eq 4–6 (described under Materials and Methods) led to the values presented in Table I. Comparative analyses of the phytochrome phototransformation with the initial rates method of Butler (1972) under standard conditions are also shown in Table I. Control experiments showed no measurable actinic effect of the measuring beam.

Discussion

The importance of studying kinetic data of photochemical interconversions over a large range of light dosage has been emphasized by Johns (1971). For this reason, our photochemical analyses of phytochrome examine the complete phototransformation process rather than just the initial 5–10%

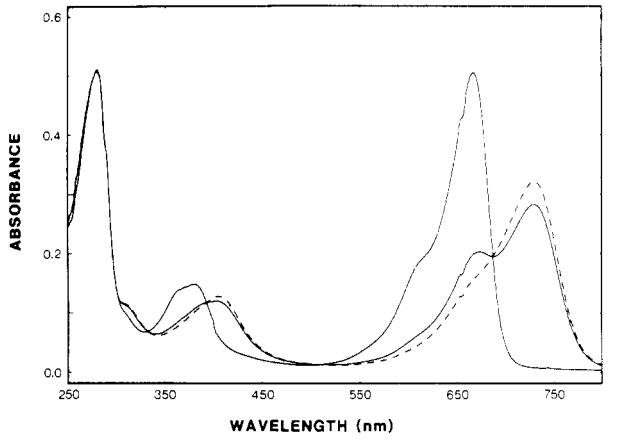

FIGURE 3: Absorbance spectra of 124-kDa *Avena* phytochrome in TEGE buffer at 5 °C. The solid lines represent the P_R form and the photoequilibrium mixture of P_R and P_{FR} forms obtained at photoequilibrium under red light (648 nm). The latter represents an equilibrium mole fraction of the P_{FR} form, $X^{FR}_{648\infty}$, of 0.876. The dashed line corresponds to the spectrum of an equimolar solution of the pure P_{FR} form obtained empirically from the photoequilibrium spectrum by subtraction of the absorbance due to the presence of 12.4% P_R and then division by 0.876. A tabular presentation of these spectra and extinction coefficients is presented in the supplementary material.

photoconversion. Most of the previous kinetic measurements of the light-driven $P_R \rightleftharpoons P_{FR}$ conversions have been based upon the initial rates method developed in 1964 by Butler, Hendricks, and Siegelman. Although photochemical cross sections can be calculated from initial rate determinations, the accuracy of these calculations is uncertain because of the difficulty in extrapolating a tangent to a curve at zero exposure (Johns, 1971). By contrast, quantum yield measurements using the approach to equilibrium derivation described in the present work are more reliable.

In practice, the validity of the present photochemical analysis of phytochrome photointerconversions must satisfy two fundamental requirements. First, an accurate measurement of the absorbed light intensity or dose is required since only absorbed light can affect the two $P_R \rightleftharpoons P_{FR}$ phototransformations. Second, experimental conditions must be chosen to ensure that the photochemical system involves only two light-absorbing species (i.e., P_R and P_{FR}) throughout the entire photoconversion process. Significant errors can be introduced in the measurements of the quantum yields and the photoequilibrium mole fraction of P_{FR} if these conditions are not satisfied. Therefore, much of the present analysis deals with intensity measurements and the development of conditions where P_R and P_{FR} are the only significant light-absorbing species.

Use of chemical actinometry allows measurement of the true absorbed intensity, inherently corrected for sample distance from the light source, noncoherence of the light beam, and light piping and reflectance by the cuvette (Lee & Seliger, 1964; Calvert & Pitts, 1967). The calibration of the photodiode array spectroradiometer provides an accurate measurement of the relative actinic light intensity throughout the spectral range from 400 to 800 nm. Combining these relative measurements with actinometry allows accurate determination of red and far-red fluence in the sample cuvette. By using these intensity determinations and the empirically derived apparent path length correction of Figure 2, we have confidence that the accurate measurement of the light dose absorbed by a phytochrome solution has been realized.

Yamamoto & Smith (1981) have emphasized the importance of assuring that phytochrome phototransformation measurements involve a two-component system. The present results underscore the importance of the choice of the actinic light intensity for the kinetic measurements of phytochrome

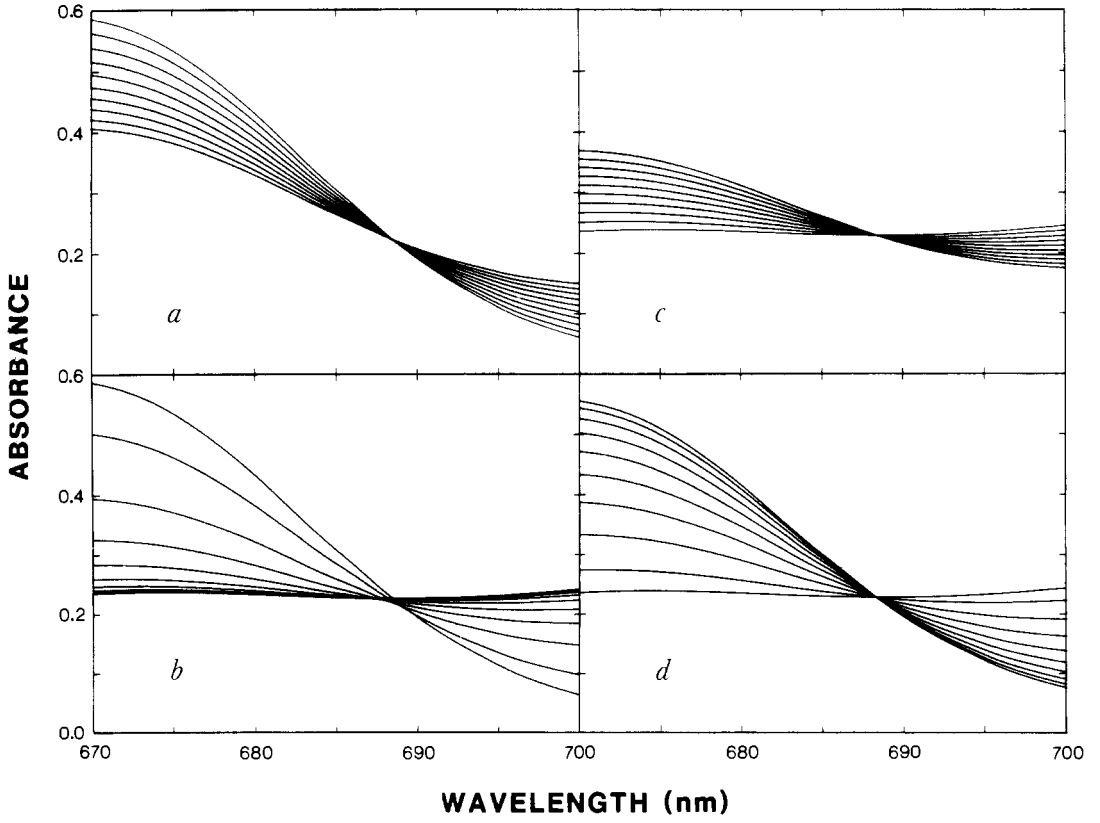

FIGURE 4: Isosbestic analysis of phytochrome phototransformations. Panels a and b represent the P_R to P_{FR} interconversion at I^i_0 values at 648 nm of 160 and 2900 pE s^{-1}, respectively. Panels c and d represent the P_{FR} to P_R interconversion at I^i_0 values at 738 nm of 200 and 3300 pE s^{-1}, respectively.

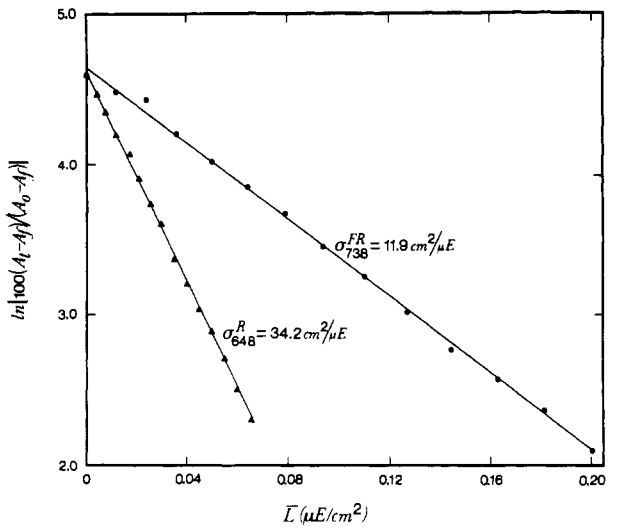

FIGURE 5: Kinetic analysis of the two phototransformations of phytochrome under standard conditions. In this specific case, 3 μM phytochrome in TEGE buffer at 5 °C was irradiated with the following incident intensities: I^i_0 = 290 pE s^{-1} at 648 nm for the P_R to P_{FR} interconversion and I^i_0 = 1100 pE s^{-1} at 738 nm for the P_{FR} to P_R interconversion. The logarithm of the percent remaining absorbance, $\ln(100[A_t - A_f)/(A_0 - A_f)])$, was plotted as a function of the absorbed fluence, $\bar{L}$ (microeinsteins per square centimeter), determined by eq 3 described under Materials and Methods.

phototransformations as shown in Figure 4. Since phototransformation intermediates may absorb light at the irradiation wavelength, their accumulation will thus contribute to the experimentally measured values of the photochemical cross sections. By use of reduced light intensities, appreciable buildup of intermediates and, therefore, erroneous values for the measured quantum yields can be avoided. As indicated by the high red light intensities seen in Table I, previous investigators have not fully appreciated the effect of transient species present during illumination on the determination of phytochrome quantum yields. Furthermore, the rate of formation of intermediates along the P_R to P_{FR} pathway will be largest under initial conditions where mostly P_R is present. Their concentration will decrease with time under continuous illumination after a significant fraction of P_{FR} is formed. For this reason, more error is potentially introduced into quantum yield measurements obtained from initial rate determinations. The contribution of the absorption of light by intermediates to the $P_R \leftrightharpoons P_{FR}$ quantum yields could therefore explain the lower quantum yield ratio, ϕ^R/ϕ^{FR}, observed by previous investigators (see Table I).

The photochemical parameters of *Avena* phytochromes obtained by previous investigators are compared with our data in Table I after recalculation of the published quantum yields by using the molar extinction coefficient of the 124-kDa species (Litts et al., 1983). Direct comparison is difficult, however, due to experimental differences in irradiation wavelengths, sample buffers, and molecular size of the phytochrome samples. Since degradation of phytochrome to smaller species is known to alter some of the spectrophotometric properties of the purified molecule (Litts et al., 1983; Vierstra & Quail, 1983b), comparison of only those results obtained with the 124-kDa species will be considered here.

The imprecision of intensity measurements is probably the major contributing factor to the observed differences between quantum yield values obtained with our method and those obtained with the method of initial rates (Table I). Indeed, we have observed much higher estimates of both ϕ^R and ϕ^{FR} using an initial rates protocol where the determination of the absorbed light fluence was less precise than that utilized for the approach to equilibrium analysis. Similarly, Vierstra & Quail (1983a) probably overestimated the absorbed light dose for their measurements, leading to a considerably reduced P_R to P_{FR} quantum yield value compared with that observed with our protocol. For this reason, comparisons between the measurements of the quantum yield ratio (ϕ^R/ϕ^{FR}) are inherently more valid since this ratio does not depend on absolute light intensity measurements. Comparison between the values of ϕ^R/ϕ^{FR} for the 124-kDa species measured by the method of initial rates reveals that our determination gives a lower estimate for this ratio than that of Vierstra & Quail (1983a). Although this difference is not large, a possible explanation is that phytochrome purified as P_{FR} (Vierstra & Quail, 1983a,b) has undergone posttranslational or posthomogenization modifications different from the P_R-purified species used in our studies. In support of this view is the recent observation that a significant conformational change of the protein structure accompanies phytochrome phototransformation in vitro (Lagarias & Mercurio, 1985), which allows for differential modification of the two forms before or after extraction. Direct comparison of P_R- and P_{FR}-purified phytochrome is needed to clarify the observed differences in photochemical properties.

The ratio of quantum yields that we obtain by the approach to equilibrium method is, however, significantly higher than that obtained by the method of initial rates. Aside from light intensity considerations raised above, one explanation for this difference is thermal dark reversion of P_{FR} to P_R which would contribute to an apparent increase in the rate of P_{FR} to P_R phototransformation. This effect would be exacerbated for the initial rates measurements which take longer to perform than the approach to equilibrium measurements. This hypothesis is reasonable for our phytochrome samples which exhibit small but measurable amounts of dark reversion; however, it is hard to reconcile with the lack of dark reversion reported by Vierstra & Quail (1983a) for their 124-kDa species. Alternatively, the observed differences in the quantum yield ratio could arise from inaccuracies in estimating the initial rate by approximating tangents to curves (Johns, 1971).

By careful light intensity measurement and by rapidly obtaining kinetic data for more complete $P_R \leftrightharpoons P_{FR}$ phototransformations, we have established that the P_R quantum yield, the ratio of quantum yields, and the extent of red light photoequilibrium of 124-kDa *Avena* phytochrome in vitro are higher than previously obtained for all molecular species of phytochrome (Table I). Since the quantum yield ratio (and hence the extent of red light photoequilibrium) obtained by Butler et al. (1964) has been used to determine phytochrome action in vivo (Pratt & Briggs, 1966), to predict the extent of photoequilibrium in vivo under polychromatic irradiation (Holmes & Fukshansky, 1979; Gardner & Graceffo, 1982), and to provide the basis for a quantitative correlation between the equilibrium concentration of P_{FR} in a plant tissue with a given physiological response (Hanke et al. 1969; Oelze-Karow & Mohr, 1973), the results presented here indicate the need for reevaluation of much of this work. Figure 6 illustrates the prediction of the wavelength dependence of $X^{FR}_{\lambda_{ss}}$ propagated from the spectra in Figure 3 and the quantum yields ratio presented in Table I. The extinction coefficients of 100% P_R and P_{FR} calculated as part of this prediction are available as supplementary material to this paper.

With regard to future investigations, it is important to note that there is variability in the range of quantum yield values obtained from sample to sample, with the value of $\phi^R_{\lambda_1}$ as low

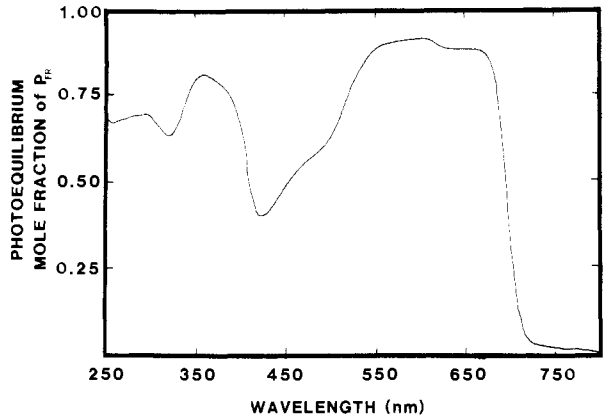

FIGURE 6: Prediction of the wavelength dependence of the mole fraction of P_{FR} at photoequilibrium under monochromatic irradiation at λ_1. $X^{FR}_{\lambda_1,eq}$ was determined by eq 5, and the experimentally determined values of the quantum yields ϕ^{R}_{λ} and ϕ^{FR}_{λ} were from Table I. This prediction represents the average of five independent absorbance spectral measurements on phytochrome obtained under the standard conditions described in Figure 5.

as 0.13 and as high as 0.17. Whether these differences arise from biochemical differences in the phytochrome sample, possibly due to the presence of unknown cofactors or covalent adducts such as chromophore X (Cha et al., 1983), or from differences in posttranslational modification remain future problems to be addressed. An understanding of these structural features and other environmental factors which influence phytochrome photoequilibrium in vitro may provide useful clues to the mechanism for the regulation of phytochrome-mediated biochemical and biophysical responses in plants.

ACKNOWLEDGMENTS

We thank Drs. Bruce A. Bonner (Department of Botany) and Gus H. Maki (Department of Chemistry), University of California, Davis, CA, and Dr. Winslow R. Briggs, Carnegie Institute of Washington, Palo Alto, CA, for their helpful discussions and repeated loans for equipment and facilities. We are also grateful to Marc Chun for the growth of tissue and Frank Mercurio and Daniel Kidd for the preparation of the phytochrome used in these studies. The editorial assistance of Donna Lagarias and the assistance of both Patricia Pennell and Dawne Smith, who typed the difficult manuscript, are gratefully acknowledged.

SUPPLEMENTARY MATERIAL AVAILABLE

Complete absorbance spectra for the 738-nm photoequilibrium (P_R spectra) and the 648-nm photoequilibrium (P_{FR} spectra) as well as extinction coefficient values for P_R and P_{FR} forms of *Avena* phytochrome. Data presented in tabular form every 2 nm between 250 and 800 nm (8 pages). Ordering information is given on any current masthead page.

REFERENCES

Butler, W. L. (1972) in *Phytochrome* (Mitrakos, K., & Shropshire, W., Eds.) pp 185–192, Academic Press, New York.

Butler, W. L., Hendricks, S. B., & Siegelman, H. W. (1964) *Photochem. Photobiol. 3*, 521.

Calvert, J. G., & Pitts, J. N., Jr. (1967) *Photochemistry*, pp 780–786, Wiley, New York.

Cha, T.-A., Maki, A. H., & Lagarias, J. C. (1983) *Biochemistry 22*, 2846.

Demas, J. N. (1973) *Anal. Chem. 45*, 992.

Gardner, G., & Graceffo, M. A. (1982) *Photochem. Photobiol. 36*, 349.

Hamai, S., & Hirayama, F. (1983) *J. Phys. Chem. 87*, 83.

Hanke, J., Hartmann, K. M., & Mohr, H. (1969) *Planta 86*, 235.

Hatchard, C. G., & Parker, C. A. (1956) *Proc. R. Soc. London, A 235*, 518.

Holmes, M. G., & Fukshansky, L. (1979) *Plant, Cell Environ. 2*, 59.

Johns, H. E. (1969) *Methods Enzymol. 16*, 253.

Johns, H. E. (1971) in *Creation and Detection of the Excited State* (Lamola, A. A., Ed.) pp 123–172, Marcel Dekker, New York.

Kendrick, R. E., & Spruit, C. J. P. (1977) *Photochem. Photobiol. 26*, 201.

Laemmli, U. K. (1970) *Nature (London) 227*, 680.

Lagarias, J. C., & Mercurio, F. M. (1985) *J. Biol. Chem. 260*, 2415.

Lee, J., & Seliger, H. H. (1964) *J. Phys. Chem. 40*, 519.

Linschitz, H., Kasche, V., Butler, W. L., & Siegelman, H. W. (1966) *J. Biol. Chem. 241*, 3395.

Litts, J. C., Kelly, J. M., & Lagarias, J. C. (1983) *J. Biol. Chem. 258*, 11025.

Oelze-Karow, H., & Mohr, H. (1973) *Photochem. Photobiol. 18*, 319.

Pratt, L. H. (1975) *Photochem. Photobiol. 22*, 33.

Pratt, L. H., & Briggs, W. R. (1966) *Plant Physiol. 41*, 467.

Pratt, L. H., Inoue, Y., & Furuya, M. (1984) *Photochem. Photobiol. 39*, 241.

Schopfer, P. (1984) in *Advanced Plant Physiology* (Wilkins, M. B., Ed.) pp 380–407, Pitman, London.

Shropshire, W., & Mohr, H. (1983) *Encycl. Plant Physiol., New Ser. 16A,B*, 832.

Song, P.-S., Chae, Q., & Gardner, J. (1979) *Biochim. Biophys. Acta 576*, 479.

Taylor, A. O., & Bonner, B. A. (1967) *Plant Physiol. 42*, 762.

Vierstra, R. D., & Quail, P. H. (1982) *Proc. Natl. Acad. Sci. U.S.A. 79*, 5272.

Vierstra, R. D., & Quail, P. H. (1983a) *Plant Physiol. 72*, 264.

Vierstra, R. D., & Quail, P. H. (1983b) *Biochemistry 22*, 2498.

Wegner, E. E., & Adamson, A. W. (1966) *J. Am. Chem. Soc. 88*, 394.

Wendler, J., Holzwarth, A. R., Braslavsky, S. E., & Schaffner, K. (1984) *Biochim. Biophys. Acta 786*, 213.

Yamamoto, K. T., & Smith, W. O., Jr. (1981) *Plant Cell Physiol. 22*, 1159.